

## Computational Study on the Reaction $\text{CH}_2\text{CH}_2 + \text{F} \rightarrow \text{CH}_2\text{CHF} + \text{H}$

Ming-Bo Zhang and Zhong-Zhi Yang\*

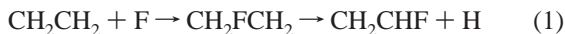
Department of Chemistry, Liaoning Normal University, Dalian, 116029, People's Republic of China

Received: February 22, 2005; In Final Form: April 7, 2005

Previous ab initio studies on reactions involving radical addition to alkenes showed that such reactions are very sensitive to theoretical levels, and thus are difficult to deal with. This motivates us to theoretically reexamine the title reaction thoroughly, which has been studied only at several low levels of theory. In the present work, the geometry optimizations and energy calculations for all species involved in the title reaction were performed at several high levels of theory. The reaction mechanism of the title reaction is discussed at the CCSD(T)/aug-cc-pVDZ//CCSD/6-31G(d,p) theoretical level. According to our study, the fluorine addition to ethylene occurs via the formation of a prereaction complex with  $C_{2v}$  symmetry, which is pointed out for the first time. The prereaction complex evolves into a fluoroethyl radical almost without a barrier, with an exothermicity of 41.49 kcal/mol. The fluoroethyl radical can further decompose into a hydrogen atom and fluoroethylene, with an energy release of 10.33 kcal/mol. Besides the direct departure of the hydrogen atom from the fluoroethyl radical, an indirect decomposition pathway may also be open, which has not been reported before. In addition, the formation of a fluoroethyl radical from a separate fluorine atom and ethylene is described pictorially via the molecular intrinsic characteristic contour (MICC) and the electron density mapped on it. Thereby, strong interpolarization and evident electron transfer between the fluorine atom and ethylene are observed as they approach each other. The transition structure for the fluorine addition to ethylene is clearly shown to be reactant-like. This provides new and intuitional insight into the title reaction.

### Introduction

The reactions of fluorine atoms with alkenes have received considerable attention, both theoretically and experimentally.<sup>1–11</sup> Lee and co-workers have performed a systematic study on the reactions between fluorine atoms with a number of olefins, using the crossed molecular beam technique.<sup>1–4</sup> It was found that this class of reactions proceeds primarily by the addition of fluorine atoms to olefins to form chemical activated radicals, which further decompose unimolecularly to give predominantly hydrogen atoms or methyl radicals. Particularly, in the reaction between a fluorine atom and ethylene, the following reaction pathway was observed:



The exothermicity of this reaction was estimated to be about  $11 \pm 2$  kcal/mol from Benson's additivity scheme.<sup>5</sup> In performing the kinematic calculations, Lee et al. found that the exoergicity of 11 kcal/mol produced a sharp nonphysical cutoff in the recoil distribution of the product and should be increased to 14 kcal/mol to produce smooth recoil distributions.<sup>4</sup> The abstraction of a hydrogen atom by a fluorine atom was another channel experimentally observed,<sup>1</sup> but the present work is primarily concerned with the formation of intermediate complexes and subsequent unimolecular decomposition; hence, the abstraction reaction is not considered.

Several ab initio theoretical studies have been carried out on the reaction between a fluorine atom and ethylene. Clark et al. located a loose transition structure for the addition of a fluorine atom to ethylene with a partial geometry optimization.<sup>9</sup> The activation barrier they obtained was 3.1 kcal/mol with respect to a separate fluorine atom and ethylene calculated at the UHF/4-31G theoretical level. Kato and Morokuma<sup>10</sup> investigated the

decomposition of  $\text{CH}_2\text{FCH}_2$  at the UHF/4-31G level of theory and obtained a loose transition structure, with an energy of 5.6 kcal/mol (5.7 kcal/mol with zero-point energy) with respect to a separate hydrogen atom and fluoroethylene. A more detailed theoretical study<sup>11</sup> on the title reaction was performed by Schlegel et al., who optimized the equilibrium geometries and transition structures and calculated their energies at several levels of theory. According to their calculations, the activation energy barrier for the addition of a fluorine atom to ethylene was less than 2 kcal/mol and the exothermicity for the title reaction was estimated to be  $15 \pm 2$  kcal/mol.

However, theoretical studies<sup>12</sup> on the reactions involving radical addition to alkenes showed that such reactions are difficult to describe theoretically and that the calculated energies are sensitive to theoretical levels. In a theoretical study of the reaction between a chlorine atom and ethylene, Braña<sup>13</sup> compared the potential energy surfaces computed at different theoretical levels and concluded that extreme care should be taken to choose an appropriate theoretical level for calculations involving radicals. However, the previous ab initio studies on the title reaction, as mentioned above, were performed at relatively low levels of theory. To our knowledge, hitherto, the highest levels used for treating the title reaction are the MP2/3-21G level for transition structure optimization and the approximate MP4/6-31G\* level for single-point energy calculation,<sup>11</sup> due to the limitation in both computational methodology and computer technique at that time. Such low levels of theory make the reliability of the computed results questionable. Thus, it is necessary to reexamine the title reaction at sophisticated levels of theory, which has been feasible only in recent years, to provide theoretical knowledge accurate enough to be useful for further kinetic and thermodynamic theoretical study.

Additionally, chemists are interested in more than the energy,

geometry, and other properties that can be obtained directly from routine ab initio calculations. They instead require that the chemical information be interpreted in a more vivid and easily understood language that can provide them with more chemical intuitions other than a pile of abstract numbers. Some efforts have already been made in this direction. For example, Bader advanced the theory of atoms in molecule (AIM),<sup>14</sup> which reflects and encodes the concept of atoms, bonds, structure, and structure stability by the topological property of the charge density and has been widely used for the analysis of chemical bonding.<sup>15</sup> Politzer et al. mapped such molecular physical properties as electrostatic potential or local ionization potential on the molecular surface corresponding to a certain electron density to analyze molecular reactivity.<sup>16</sup> In analogy to Politzer's idea, Ehresmann et al. defined local electron affinity, electronegativity, and hardness and projected them onto molecular isodensity surfaces to describe acceptor and other electronic properties on molecular surfaces or in the vicinity of molecules.<sup>17</sup> Mezey and co-workers employed molecular isodensity contour (MIDCO) to describe molecular shape and molecular similarity based on it.<sup>18</sup> Furthermore, they explored the correlations between molecular chemical properties such as toxicity and drug activity with topological character of molecular shape.<sup>19–21</sup> Recently, Yang et al. have developed a new method for representing molecular shape, the molecular intrinsic characteristic contour (MICC), based on the potential acting on an electron in a molecule (PAEM).<sup>22–24</sup> They have explored the shape changing during the process of  $\text{H}_2$  forming from two separate hydrogen atoms in terms of MICC.<sup>22</sup> More recently, they have investigated the polarization and bonding interaction pictures between a hydrogen atom and a fluorine atom via the model of MICC and the electron density mapped on it.<sup>23</sup> In this work, we will present a variation of the MICC and the electron density mapped on the contour along the reaction pathway for the formation of  $\text{CH}_2\text{FCH}_2$  from a separate fluorine atom and ethylene, for the purpose of providing a new and vivid description of this chemical reaction.

The work is organized as follows. In the next section, we present the computational details employed in this work. The third section contains (1) an ab initio study of the potential energy surface (PES) for the title reaction and (2) a brief introduction to the definition of the PAEM and the MICC for the sake of completeness, which have been described in detail elsewhere.<sup>22–24</sup> In addition, the changing pictures of the MICC and the electron density on the contour for a series of structures involved in the formation of  $\text{CH}_2\text{FCH}_2$  are also presented in this section. In the last section, some conclusions of interest are given.

## Computational Details

The geometries for all species involved in the title reaction were optimized at different levels of theory. The effect of basis set on the geometrical parameters was examined by means of optimizing the structures of interest with the second-order Møller–Plesset perturbation theory (MP2)<sup>25</sup> in conjunction with different basis sets, that is, Pople's<sup>26</sup> 6-31G(d,p), 6-311++G(d,p), and 6-311G++(3df,3pd) basis sets and Dunning's<sup>27</sup> aug-cc-pVDZ basis set. In addition, coupled cluster theory including single and double substitutions (CCSD)<sup>28–30</sup> with the 6-31G(d,p) basis set was also utilized for geometrical optimization with the aim to examine the influence of electronic correlation on the geometrical parameters. Vibrational frequencies were calculated at the MP2/6-311++G(d,p) level to identify the obtained stationary points as either equilibrium structures or

transition states. To improve the energy prediction, the CCSD(T)<sup>31</sup> method with the aug-cc-pVDZ basis set was used to calculate the single-point energies based on the geometries of the MP2/6-311++G(3df,3pd) and CCSD/6-31G(d,p) levels, respectively. The zero-point energies (ZPEs) for all structures were calculated at the MP2/6-311++G(d,p) level and not scaled. All these calculation works were performed with the Gaussian 98 program.<sup>32</sup>

The potential acting on an electron in a molecule (PAEM) was calculated by the configuration interaction with all single and double substitutions (SDCI) method in conjunction with the 6-31+G(d,p) basis set. The calculation was performed using the ab initio MELD<sup>33</sup> program and a separate code developed by us. According to the definition of the MICC, to be discussed later, to determine the MICC, knowledge of the ionization potentials for the structures considered is required. In this work, a vertical ionization potential was adopted and calculated at the CCSD(T)/aug-cc-pVDZ//MP2/6-311++G(3df,3pd) level using the Gaussian 98 program. Visualization of the MICCs was achieved using the free code (SCILAB 2.6).<sup>34</sup>

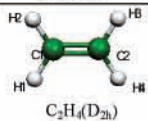
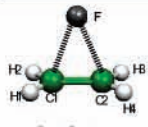
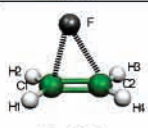
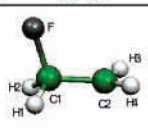
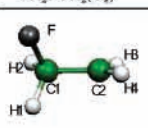
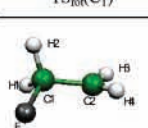
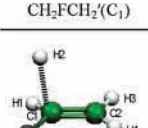
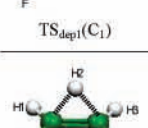
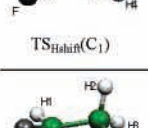
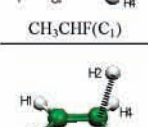
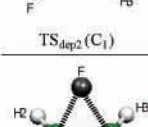
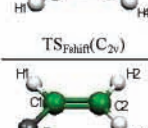
## Results and Discussion

**1. Ab Initio Study on the Potential Energy Surface (PES) for the Title Reaction.** *1.1. Geometries.* All of the structures located in this work are presented in Table 1, including the reactants, prereaction complexes, intermediates, transition structures, and products. For the sake of simplicity, we list only the most representative parameters for these structures as computed at the different levels of theory employed in this work.

Comparison of the geometries obtained with the MP2 method in conjunction with different basis sets allows us to examine the effects of basis sets on the geometrical parameters. Generally, the MP2 method with Pople's series of basis sets provides similar geometries. The discrepancies in bond lengths are within 0.022 Å for the C–C bond, 0.015 Å for the C–H bond, and 0.023 Å for the C–F bond. The largest discrepancies in C–C, C–H, and C–F bond lengths occur in the transition structure  $\text{TS}_{\text{Fshift}}$ , the transition structure  $\text{TS}_{\text{dep1}}$ , and the prereaction complex ( $\mathbf{I}_{\text{add}}$ ), respectively, implying that the geometrical parameters of the transition structures and weakly bound complex ( $\mathbf{I}_{\text{add}}$ ) are more sensitive to the sizes of basis sets. As to Dunning's aug-cc-pVDZ basis set, it usually renders bond lengths longer than those of Pople's basis sets but similar bond angles and dihedral angles. Note that the most remarkable discrepancy between Dunning's aug-cc-pVDZ basis set and Pople's basis sets occurs in the structure of  $\text{CH}_2\text{FCH}_2'$ , which is located using the MP2 method with Pople's basis sets as an equilibrium structure, and is unstable with respect to the rotation around the C–C bond at the MP2/aug-cc-pVDZ level. Accordingly, the transition structure  $\text{TS}_{\text{rot}}$  connecting the two conformers,  $\text{CH}_2\text{FCH}_2$  and  $\text{CH}_2\text{FCH}_2'$ , cannot be obtained at the MP2/aug-cc-pVDZ level either. Since the results of electron spin resonance (ESR) experiments<sup>35</sup> show the existence of at least two conformers for the fluoroethyl radical, Pople's basis sets are preferred over Dunning's aug-cc-pVDZ basis set for the geometrical optimization in the study of the title reaction.

Comparison of geometries optimized at the CCSD/6-31G(d,p) level with those at the MP2/6-31G(d,p) level shows that the increase in electron correlation has no apparent impact on the equilibrium structures, with the exception of the weakly bound complex ( $\mathbf{I}_{\text{add}}$ ), as shown in Table 1. For all of the bond lengths in these structures, the typical discrepancies detected are within 0.006 Å. However, in the case of transition structures involving bond forming or breaking and the complex  $\mathbf{I}_{\text{add}}$ , the

**TABLE 1: Representative Geometrical Parameters for All Structures Involved in the Title Reaction as Computed at Different Theoretical Levels**

SYSTEM	PARAMETERS	MP2				CCSD
		6-31G (d,p)	6-311++G (d,p)	6-311++G (3df,3pd)	Aug-cc -pVDZ	6-31G (d,p)
 C <sub>2</sub> H <sub>4</sub> (D <sub>2h</sub> )	R <sub>C1-C2</sub> R <sub>C1-H1</sub> A <sub>H1-C1-C2</sub>	1.335 1.081 121.6	1.339 1.086 121.5	1.332 1.081 121.3	1.349 1.093 121.3	1.336 1.082 121.6
 I <sub>add</sub> (C <sub>2v</sub> )	R <sub>C1-C2</sub> R <sub>C1-F</sub> R <sub>C1-H1</sub> A <sub>C2-C1-F</sub> A <sub>H1-C1-C2</sub> D <sub>H1-C1-C2-H3</sub>	1.377 1.935 1.078 69.0 121.0 175.7	1.387 1.953 1.082 69.2 120.6 176.7	1.382 1.930 1.077 69.2 120.6 176.9	1.397 1.947 1.090 69.0 120.7 177.0	1.358 2.088 1.080 71.0 121.4 178.0
 TS <sub>add</sub> (C <sub>s</sub> )	R <sub>C1-C2</sub> R <sub>C1-F</sub> R <sub>C2-F</sub> R <sub>C1-H1</sub> A <sub>C2-C1-F</sub> A <sub>H1-C1-C2</sub> D <sub>H1-C1-C2-H3</sub>	1.355 1.842 1.950 1.078 73.4 121.2 175.6	1.369 1.859 1.978 1.082 73.8 120.8 176.4	1.367 1.846 1.960 1.077 73.5 120.7 176.8	1.382 1.859 1.978 1.089 73.5 120.7 176.9	1.356 2.063 2.099 1.080 72.5 121.4 178.0
 CH <sub>2</sub> FCH <sub>2</sub> (C <sub>s</sub> )	R <sub>C1-C2</sub> R <sub>C1-F</sub> R <sub>C1-H1</sub> A <sub>H1-C1-C2</sub> A <sub>C2-C1-F</sub> D <sub>F-C1-C2-H1</sub>	1.483 1.410 1.090 111.4 110.4 119.1	1.485 1.411 1.092 111.7 110.1 118.3	1.479 1.405 1.087 111.9 110.1 118.3	1.488 1.433 1.099 112.3 109.8 117.7	1.487 1.409 1.091 111.5 110.3 119.0
 TS <sub>rot</sub> (C <sub>1</sub> )	R <sub>C1-C2</sub> R <sub>C1-F</sub> R <sub>C1-H2</sub> R <sub>C2-H3</sub> A <sub>C2-C1-F</sub> D <sub>H2-C1-C2-H3</sub>	1.482 1.407 1.089 1.077 110.4 7.3	1.484 1.405 1.092 1.081 110.2 5.6	1.478 1.402 1.087 1.076 110.3 9.2		1.487 1.405 1.090 1.079 110.4 7.2
 CH <sub>2</sub> FCH <sub>2</sub> (C <sub>1</sub> )	R <sub>C1-C2</sub> R <sub>C1-F</sub> R <sub>C1-H2</sub> R <sub>C1-H1</sub> A <sub>H2-C1-C2</sub> A <sub>C2-C1-F</sub>	1.481 1.398 1.096 1.092 112.0 110.1	1.483 1.398 1.098 1.093 112.0 110.3	1.476 1.390 1.094 1.090 112.0 110.4		1.485 1.396 1.097 1.093 112.0 110.0
 TS <sub>dip1</sub> (C <sub>1</sub> )	R <sub>C1-C2</sub> R <sub>C1-H2</sub> R <sub>C1-F</sub> A <sub>H2-C1-C2</sub> D <sub>H2-C1-C2-F</sub> D <sub>H3-C1-C2-F</sub>	1.334 1.792 1.354 102.0 105.7 175.9	1.332 1.791 1.348 102.1 104.2 175.9	1.325 1.777 1.340 112.0 104.1 175.8	1.339 1.799 1.365 102.0 103.5 175.8	1.350 1.855 1.355 102.5 105.8 176.3
 TS <sub>Hahn</sub> (C <sub>1</sub> )	R <sub>C1-C2</sub> R <sub>C1-H2</sub> R <sub>C1-F</sub> R <sub>C2-H2</sub> A <sub>C2-C1-H2</sub> D <sub>H2-C1-C2-F</sub>	1.465 1.275 1.373 1.301 56.2 114.3	1.466 1.287 1.366 1.309 56.3 113.3	1.460 1.283 1.358 1.302 56.2 113.8	1.471 1.295 1.385 1.317 56.4 114.4	1.472 1.295 1.371 1.316 56.4 114.2
 CH <sub>3</sub> CHF(C <sub>1</sub> )	R <sub>C1-C2</sub> R <sub>C2-H2</sub> R <sub>C1-F</sub> R <sub>C2-H4</sub> D <sub>H2-C1-C2-F</sub>	1.482 1.094 1.362 1.089 65.3	1.484 1.098 1.356 1.093 64.4	1.477 1.094 1.348 1.088 64.0	1.489 1.106 1.375 1.101 64.4	1.486 1.110 1.360 1.090 65.3
 TS <sub>dip2</sub> (C <sub>1</sub> )	R <sub>C1-C2</sub> R <sub>C1-F</sub> R <sub>C2-H2</sub> A <sub>C1-C2-H2</sub> D <sub>F-C1-C2-H3</sub>	1.327 1.349 1.841 108.52 173.9	1.326 1.343 1.850 107.9 174.6	1.319 1.335 1.837 107.1 175.4	1.334 1.360 1.858 107.1 175.5	1.344 1.351 1.926 107.8 174.5
 TS <sub>Hahn</sub> (C <sub>2v</sub> )	R <sub>C1-C2</sub> R <sub>C1-F</sub> R <sub>C1-H1</sub> A <sub>C2-C1-F</sub> D <sub>F-C1-C2-H1</sub>	1.614 1.673 1.077 57.7 82.8	1.601 1.674 1.079 57.2 84.3	1.592 1.661 1.075 57.2 84.8	1.615 1.689 1.088 61.4 83.5	1.578 1.795 1.077 64.0 84.0
 CH <sub>2</sub> CHF(C <sub>s</sub> )	R <sub>C1-C2</sub> R <sub>C1-H1</sub> R <sub>C2-H3</sub> R <sub>C1-F</sub> A <sub>F-C1-C2</sub>	1.328 1.081 1.078 1.354 122.1	1.330 1.084 1.083 1.348 121.7	1.324 1.080 1.078 1.341 122.1	1.339 1.091 1.090 1.365 121.7	1.328 1.081 1.079 1.354 121.8

**TABLE 2: Single-Point Energies and Those Including Zero-Point Energy Correction in Parentheses as Well as Zero-Point Energy (Relative to  $\text{CH}_2\text{CH}_2 + \text{F}$ , in kcal/mol) for the Prereaction Complex, Intermediates, Transition Structures, and Products as Computed at Different Levels of Theory**

system	MP2/6-311++ G(3df,3pd) <sup>a</sup>	PMP2/6-311++ G(3df,3pd) <sup>a</sup>	CCSD/6-31G(d,p) <sup>b</sup>	CCSD(T)/ aug-cc-pVDZ <sup>a</sup>	CCSD(T)/ aug-cc-pVDZ <sup>b</sup>	ZPE <sup>c</sup>
<b>I<sub>add</sub></b>	-17.35	-18.42	-5.33	-13.77 (-8.76)	-14.31 (-9.30)	5.01
<b>TS<sub>add</sub></b>	-15.73	-18.80	-5.24	-13.47 (-10.87)	-14.28 (-11.68)	2.60
<b>CH<sub>2</sub>FCH<sub>2</sub></b>	-51.31	-51.62	-41.59	-43.59 (-41.38)	-43.70 (-41.49)	2.21
<b>TS<sub>rot</sub></b>	-51.29	-51.62	-41.54	-43.51 (-41.68)	-43.63 (-41.80)	1.83
<b>CH<sub>2</sub>FCH<sub>2</sub>'</b>	-51.44	-51.78	-41.82	-43.40 (-41.55)	-43.55 (-41.70)	1.85
<b>TS<sub>dep1</sub></b>	-5.52	-11.97	3.05	-0.74 (-3.12)	-1.82 (-4.20)	-2.38
<b>CH<sub>3</sub>CHF</b>	-55.45	-55.62	-46.31	-46.50 (-44.05)	-46.77 (-44.32)	2.45
<b>TS<sub>Hshift</sub></b>	-6.43	-8.60	7.79	2.67 (2.17)	2.20 (1.70)	-0.50
<b>TS<sub>dep2</sub></b>	-7.87	-14.03	0.61	-2.59 (-4.97)	-3.63 (-6.01)	-2.38
<b>TS<sub>Fshift</sub></b>	54.98	48.06	58.15	26.05 (26.62)	9.03 (9.60)	0.57
H CH <sub>2</sub> CHF }	-17.47	-16.47	-4.07	-5.90 (-10.08)	-6.15 (-10.33)	-4.18

<sup>a</sup> Single-point calculation on the MP2/6-311++G(3df,3pd) geometries. <sup>b</sup> Single-point calculation on the CCSD/6-31G(d,p) geometries. <sup>c</sup> Zero-point energy (ZPE) calculated at the MP2/6-311++G(d,p) level.

discrepancies are considerably large. For example, the bond length  $R_{\text{C1-F}}$  in **I<sub>add</sub>** changes from 2.088 Å computed at the CCSD/6-31G(d,p) level to 1.935 Å computed at the MP2/6-31G(d,p) level. Likewise, the bond length  $R_{\text{C1-H2}}$  in **TS<sub>dep2</sub>** obtained at the CCSD/6-31G(d,p) level is 0.085 Å longer than that at the MP2/6-31G(d,p) level.

It is worth noting that in the transition structure **TS<sub>add</sub>** for the fluorine addition to ethylene, the angle between the C1-C2 bond and the C1-F bond (i.e.,  $A_{\text{F-C1-C2}}$  in **TS<sub>add</sub>**) is about 73° obtained by us at the MP2/6-31G(d,p) level, consistent with the results obtained at higher levels of theory such as the MP2/6-311++G(3df,3pd) and CCSD/6-31G(d,p) levels (see Table 1). However, in the transition structure obtained by Schlegel<sup>11a</sup> at relatively lower levels of theory, including HF/3-21G, HF/6-31G\*, and MP2/3-21G, the angle was predicted to be ~105°, substantially distinct from that obtained by us. Thus, it seems that MP2/6-31(d,p) is the lowest level of theory to obtain reliable geometrical parameters for the structures involved in the title reaction. Note that such differences in geometry will lead to different reaction mechanisms, as discussed below.

In conclusion, for systems similar to the title reaction, the geometrical parameters for weakly bound structures and transition structures are more sensitive to theoretical level than other equilibrium structures. To obtain reliable geometrical parameters, the MP2/6-31(d,p) level of theory or higher is needed.

**1.2. Energetics and Reaction Mechanism.** Previous studies on the addition of a radical to alkenes have shown that the energetics of such reactions are very sensitive to theoretical levels.<sup>11-13</sup> Thus, we calculated the energies at several levels for the purpose of comparison. The calculated results are summarized in Table 2.

To test the effect of spin contamination on the energetics, we present in Table 2 the relative energies calculated at the MP2/6-311++G(3df,3pd) level and the corresponding spin-projected energy (PMP2), respectively. It can be seen that, for the equilibrium structures, the MP2 and PMP2 methods provide similar relative single-point energies with typical discrepancies within 1.0 kcal/mol. However, for the transition structures including **TS<sub>add</sub>**, **TS<sub>dep1</sub>**, **TS<sub>dep2</sub>**, and **TS<sub>Fshift</sub>**, projecting out the spin contamination reduces the relative energy of MP2 considerably, with the largest amount up to 7.0 kcal/mol. This indicates that these transition structures suffer a more serious spin contamination than the equilibrium structures. Consequently, the MP2 method tends to overestimate barrier height. Thus, the annihilation of the spin contamination from unrestricted wave functions is mandatory for calculations on barrier heights in the present work.

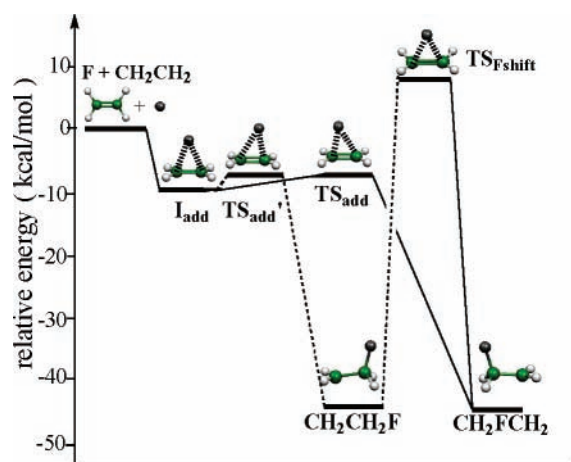


**Figure 1.** Energy variations along the reaction pathways for the fluorine addition to ethylene.

Stanton has shown that all spin contamination is essentially removed from a coupled cluster wave function.<sup>36</sup> Chuang et al. have also shown that coupled cluster methods, even with unrestricted reference states, provide good approximations to transition state geometries and energies for radical reactions.<sup>37</sup> Thus, in this work, we calculated the relative energies at the CCSD(T)/aug-cc-pVDZ level based on the geometries of MP2/6-311++G(3df,3pd) and CCSD/6-31G(d,p), respectively. In general, the relative single-point energies without ZPE correction obtained at the two levels agree well with each other, with the typical deviations within 1.0 kcal/mol, as shown in Table 2. However, the transition structure **TS<sub>Fshift</sub>** is an evident exception, where the energy difference between two geometries is up to about 17.0 kcal/mol. Over all, it seems that the MP2 method with a large basis set may yield geometries with a quality close to that obtained by a highly correlated calculation with a modest basis set, from the viewpoint of energetics.

On the basis of the geometries and energies obtained, the reaction mechanism for the substitution reaction of a fluorine atom with ethylene can be determined. In the following, we will discuss the reaction mechanism based on the results of CCSD(T)/aug-cc-pVDZ//CCSD/6-31G(d,p) including ZPE correction obtained at the MP2/6-311++G(d,p) level, unless otherwise stated.

**A. Formation of the Fluoroethyl Radical.** We present the possible reaction pathways for the fluorine addition to ethylene in Figure 1. As the fluorine atom and ethylene approach each other, the fluorine atom associates with ethylene to form a

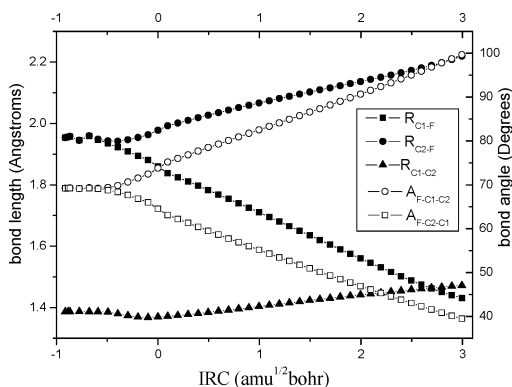


**Figure 2.** Changes of bond lengths and bond angles along the IRC calculated at the MP2/6-311++G(d,p) level.

prereaction complex,  $\mathbf{I}_{\text{add}}$  ( ${}^2A_1$ ), which then evolves into  $\text{CH}_2\text{-FCH}_2$  via a transition structure,  $\mathbf{TS}_{\text{add}}$ . The prereaction complex ( $\mathbf{I}_{\text{add}}$ ) exhibits  $C_{2v}$  symmetry, where the fluorine atom lies along the  $C_2$  axis, with the bond lengths  $R_{\text{C1-F}}$  and  $R_{\text{C2-F}}$  equal to 2.088 Å. The association of a fluorine atom to ethylene elongates the C1–C2 bond of ethylene by 0.022 Å, as shown in Table 1. This indicates that the presence of a fluorine atom weakens the C–C  $\pi$  bond to a certain degree, which may be attributed to the electron donation from the filled  $\pi$  orbital of ethylene to the empty p orbital of fluorine. In the transition structure for the addition of a fluorine atom to ethylene ( $\mathbf{TS}_{\text{add}}$ ), the fluorine atom gets closer to one of the carbons (C1, in the present case), simultaneously getting farther from the other carbon (C2). By comparing the geometry of  $\mathbf{TS}_{\text{add}}$  with those of  $\mathbf{I}_{\text{add}}$  and  $\text{CH}_2\text{-FCH}_2$ , it can be clearly seen that the geometry of  $\mathbf{TS}_{\text{add}}$  is close to that of the reactant  $\mathbf{I}_{\text{add}}$ , thus an early transition structure.

According to Schlegel's calculations, the bond angle  $A_{\text{F-C1-C2}}$  ( $\sim 105^\circ$ ) in the transition structure  $\mathbf{TS}_{\text{add}}$  is close to that ( $\sim 110^\circ$ ) in  $\text{CH}_2\text{FCH}_2$ .<sup>11a</sup> As a result, on the PES obtained by Schlegel, the fluorine atom and ethylene reach the transition structure directly from a separate fluorine atom and ethylene without the presence of the prereaction complex ( $\mathbf{I}_{\text{add}}$ ), which is in disagreement with our conclusion. To confirm involvement of the complex  $\mathbf{I}_{\text{add}}$  in the title reaction, an intrinsic reaction coordinate (IRC)<sup>38,39</sup> calculation was performed starting from the transition state  $\mathbf{TS}_{\text{add}}$  at the MP2/6-311++G(d,p) level. The variations of geometrical parameters closely relevant to the reaction coordinate along the IRC are shown in Figure 2. It can be seen that, at  $-1$  ( $\text{amu})^{1/2}\text{bohr}$ , the bond length  $R_{\text{C1-F}}$  and the bond angle  $A_{\text{F-C1-C2}}$  are nearly identical to  $R_{\text{C2-F}}$  and  $A_{\text{F-C2-C1}}$ , respectively. Going along the IRC, the bond length  $R_{\text{C1-F}}$  decreases, accompanied by an increase in the bond angle  $A_{\text{F-C1-C2}}$ ; correspondingly, the bond length  $R_{\text{C2-F}}$  becomes longer and the bond angle  $A_{\text{F-C2-C1}}$  gets smaller, indicating the formation of the C1–F bond. At the same time,  $R_{\text{C1-C2}}$  initially decreases slightly and then begins to increase, reflecting the conversion of the carbon double bond to a single bond. Thus, in terms of the IRC calculation, it can be concluded that the transition structure  $\mathbf{TS}_{\text{add}}$  indeed starts from the prereaction structure ( $\mathbf{I}_{\text{add}}$ ) rather than a separate fluorine atom and ethylene and proceeds toward the formation of  $\text{CH}_2\text{FCH}_2$ .

As has been indicated earlier, most radical additions to the unsaturated carbon–carbon double bond have negative activation barriers.<sup>12,40–43</sup> Our calculations predict that the transition structure for the fluorine addition to ethylene ( $\mathbf{TS}_{\text{add}}$ ) is lower in energy than that of the separate fluorine atom and ethylene, at all levels of theory employed. Thus, the presence of  $\mathbf{I}_{\text{add}}$  on the PES is mandatory, for the topological consistency of the PES of the title reaction. Furthermore, in the crossed molecular

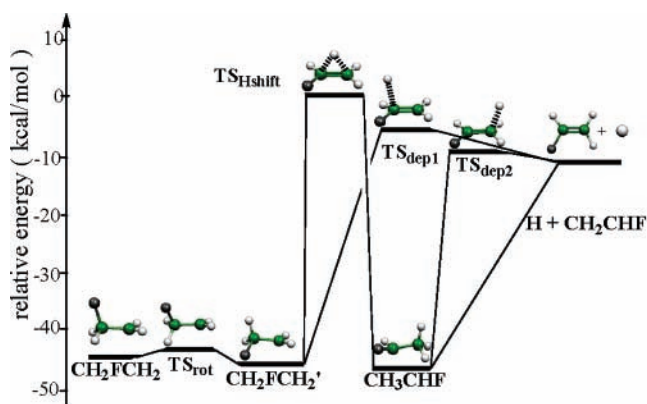


**Figure 3.** Energy variations along the possible reaction pathways for the reaction  $\text{CH}_2\text{FCH}_2 \rightarrow \text{CH}_2\text{CHF} + \text{H}$ .

beam study, Parson and Lee observed that if the fluorine atom approaches ethylene in a direction perpendicular to the molecular plane of ethylene, it is favorable for the formation of a collision complex.<sup>1</sup> The involvement of  $\mathbf{I}_{\text{add}}$  with  $C_{2v}$  symmetry may be responsible for such regioselectivity observed. To our knowledge, it is the first time that the existence of a prereaction complex in the title reaction has been reported.

The energy of  $\mathbf{TS}_{\text{add}}$  computed at the CCSD(T)/aug-cc-pVDZ//CCSD/6-31G(d,p) level is 0.03 kcal/mol higher than that of  $\mathbf{I}_{\text{add}}$  (without ZPE correction). However, inclusion of ZPE correction lays the energy of  $\mathbf{I}_{\text{add}}$  above that of  $\mathbf{TS}_{\text{add}}$  by about 2.0 kcal/mol, suggesting that  $\mathbf{I}_{\text{add}}$  can evolve into  $\text{CH}_2\text{FCH}_2$  without a barrier. No experimental value for the energy barrier of fluorine addition to ethylene is available, but the result can be checked indirectly by comparison with the results for the reactions of other halogens with ethylene. Experimental study suggested that, in the case of chlorine and bromine, the addition to ethylene appears to have no barrier.<sup>44</sup> Since fluorine is more electronegative than chlorine and bromine, consequently, for the addition to electron-rich ethylene, the fluorine should proceed more readily than chlorine and bromine. Thus, it is reasonable to conclude that the addition of a fluorine atom to ethylene is almost free of a barrier.

The formation of  $\text{CH}_2\text{FCH}_2$  is exothermic, with an energy release of 41.49 kcal/mol calculated at the CCSD(T)/aug-cc-pVDZ//CCSD/6-31 g(d,p) level with the ZPE correction, lower than the theoretical evaluation ( $47 \pm 2$  kcal/mol) of Schlegel et al.<sup>11b</sup>

Of course, for the fluorine addition to ethylene, it is also possible that the fluorine atom is bonded to the other carbon (C2) through the transition structure  $\mathbf{TS}'_{\text{add}}$ , which is a mirror image of  $\mathbf{TS}_{\text{add}}$ , yielding  $\text{CH}_2\text{CH}_2\text{F}$ , an equivalent conformation of  $\text{CH}_2\text{FCH}_2$ . Energetically, this pathway is entirely parallel with the case of fluorine bonding to the carbon C1. The two conformations of the fluoroethyl radical are connected through a  $C_{2v}$  transition structure,  $\mathbf{TS}_{\text{Fshift}}$  ( ${}^2B_2$ ), for the shift of a fluorine atom from one carbon to the other, where the bond lengths  $R_{\text{C1-F}}$  and  $R_{\text{C2-F}}$  both are 1.795 Å. The energy of  $\mathbf{TS}_{\text{Fshift}}$  is 51.09 kcal/mol higher than that of  $\text{CH}_2\text{FCH}_2$ . Such a high energy of  $\mathbf{TS}_{\text{Fshift}}$  means that the direct interconversion between the two conformations is less likely to occur.

Note that, due to the chemical indistinguishability between  $\text{CH}_2\text{FCH}_2$  and  $\text{CH}_2\text{CH}_2\text{F}$ , mirror-symmetric are the PESs for their decomposition reactions. Thus, we consider only the PES for the decomposition of  $\text{CH}_2\text{FCH}_2$  below.

**B. Rotation around the Carbon Bond.** The possible reaction pathways for the decomposition of  $\text{CH}_2\text{FCH}_2$  are shown in Figure 3. There are two conformers for the fluoroethyl radical,

$\text{CH}_2\text{FCH}_2$  and  $\text{CH}_2\text{FCH}_2'$ , with  $C_s$  and  $C_1$  symmetry, respectively, as shown in Table 1. The conformer  $\text{CH}_2\text{FCH}_2'$  is slightly more stable than  $\text{CH}_2\text{FCH}_2$  by 0.21 kcal/mol. The two conformers are connected via a transition structure,  $\text{TS}_{\text{rot}}$ , for the rotation of the  $\text{CH}_2$  group around the C–C bond, where H1 and H3 are nearly coplanar with the two carbon atoms, with a distortion angle of several degrees. For the calculations of the rotation potential energy, only the MP2/6-311++G(3df,3pd) and CCSD/6-31G(d,p) levels show that an energy barrier exists for the rotation around the C–C bond, 0.02 and 0.05 kcal/mol, respectively (see Table 2). A calculation performed at the CCSD(T)/aug-cc-pVDZ//CCSD/6-31G(d,p) level including the ZPE correction renders the energy of  $\text{TS}_{\text{rot}}$  lower than both conformers. This indicates that the rotation around the C–C bond is nearly barrierless, which is consistent with the result obtained at the MP2/6-311\*\*//6-31G\* level by Chen et al.<sup>45</sup>

**C. Departure of a Hydrogen Atom.** The exothermicity of the formation of the fluoroethyl radical makes it an energized species which can further decompose into a hydrogen atom and fluoroethylene. The bond length  $R_{\text{C1-H2}}$  in  $\text{CH}_2\text{FCH}_2'$  is longer than  $R_{\text{C1-H1}}$  by 0.004 Å, which has been rationalized by a weak three-electron hyperconjugative interaction in the works of Schlegel<sup>11a</sup> and Chen.<sup>45</sup> Such elongation makes it more readily break than other C–H bonds. In the transition structure  $\text{TS}_{\text{dep1}}$  for the departure of a hydrogen atom, the bond length  $R_{\text{C1-H2}}$  is lengthened by 0.758 Å relative to that in  $\text{CH}_2\text{FCH}_2'$ . The energy of  $\text{TS}_{\text{dep1}}$  is 37.50 kcal/mol higher than that of  $\text{CH}_2\text{FCH}_2'$  but lower than the energy of a separate fluorine atom and ethylene by 4.20 kcal/mol. Thus, it can be well understood why the resulting fluoroethyl radical is ready to decompose even at low collision energy in the crossed molecular beam experiment.<sup>4</sup> Comparison of the energy of  $\text{TS}_{\text{dep1}}$  to that of  $\text{CH}_2\text{CHF}$  and H allows us to estimate the reverse addition barrier to be 6.13 kcal/mol, in good agreement with the estimation (5.6 ± 0.5 kcal/mol) of Schlegel et al.<sup>11b</sup>

The departure of a hydrogen atom from  $\text{CH}_2\text{FCH}_2'$  may also proceed in an indirect way, where initially the hydrogen atom H2 in  $\text{CH}_2\text{FCH}_2'$  shifts from one carbon (C1) to another carbon (C2) via the transition structure  $\text{TS}_{\text{Hshift}}$ . The energy of  $\text{TS}_{\text{Hshift}}$  is 43.40 kcal/mol higher than that of  $\text{CH}_2\text{FCH}_2'$ . The resulting isomer  $\text{CH}_3\text{CHF}$  is more stable than  $\text{CH}_2\text{FCH}_2'$  by 2.62 kcal/mol.  $\text{CH}_3\text{CHF}$  may further undergo dissociation into H and  $\text{CH}_2\text{CHF}$  via the transition structure  $\text{TS}_{\text{dep2}}$ , overcoming an energy barrier of 38.31 kcal/mol. In this indirect pathway,  $\text{CH}_2\text{FCH}_2' \rightarrow \text{TS}_{\text{Hshift}} \rightarrow \text{CH}_3\text{CHF} \rightarrow \text{TS}_{\text{dep2}} \rightarrow \text{H} + \text{CH}_2\text{CHF}$ , the migration of a hydrogen atom has a higher energy barrier and thus is a controlling step. Since the energy of  $\text{TS}_{\text{Hshift}}$  is 5.90 kcal/mol higher than that of  $\text{TS}_{\text{dep1}}$ , the indirect pathway may only play a minor role in the decomposition of  $\text{CH}_2\text{FCH}_2'$ . However, it is worthwhile to note that the energy of  $\text{TS}_{\text{Hshift}}$  (1.70 kcal/mol, relative to a separate fluorine atom and ethylene) is less than the collision energy ranging from 2.2 to 12.1 kcal/mol in the crossed molecular beam experiment.<sup>4</sup> Under this condition, the indirect decomposition pathway is also energetically accessible.

**2. Changing Pictures of the MICC and the Electron Density Mapped on It during the Formation of the Fluoroethyl Radical.** **2.1. Potential Acting on an Electron in a Molecule.** We first introduce the potential acting on an electron in a molecule (PAEM) on which the definition of the molecular intrinsic characteristic contours (MICCs) is based. Supposing that an electron in a molecule is in the electronic ground state,

**TABLE 3: Vertical Ionization Potentials (IPs) for the Structures of Interest (in hartrees)**

structure	$\text{CH}_2\text{CH}_2$	$R_d = 8.0$	$R_d = 5.9$	$\mathbf{I}_{\text{add}}$	$\mathbf{TS}_{\text{add}}$	$\text{CH}_2\text{FCH}_2$
IPs	0.3887	0.3625	0.3806	0.3215	0.3198	0.3576

the potential acting on it can be expressed as

$$V(\mathbf{r}_1) = - \sum_A \frac{Z_A}{r_{1A}} + \frac{1}{\rho(\mathbf{r}_1)} \int \frac{\rho_2(\mathbf{r}_1, \mathbf{r}_2)}{|\mathbf{r}_1 - \mathbf{r}_2|} d\mathbf{r}_2 \quad (2)$$

in which the first term is the attractive potential due to all nuclei and the second term is the repulsive potential created by other electrons in the system;  $Z_A$  is the nuclear charge of atom A,  $r_{1A}$  is the distance between the electron considered and the nucleus A, the summation involving index A is over all atomic nuclei,  $\rho(\mathbf{r}_1)$  represents the one-electron density of an electron appearing at position  $\mathbf{r}_1$ , and  $\rho(\mathbf{r}_1, \mathbf{r}_2)$  is the two-electron density function, the probability of finding one electron at  $\mathbf{r}_1$  and at the same time another electron at  $\mathbf{r}_2$ . In the configuration interaction (CI) method,  $\rho(\mathbf{r}_1)$  and  $\rho(\mathbf{r}_1, \mathbf{r}_2)$  can be specifically expressed as a combination of molecular integrations obtainable by the ab initio method. The detailed expression can be found elsewhere.<sup>23</sup>

**2.2. Definition of the Molecular Intrinsic Characteristic Contour (MICC).** The model can be formulated as follows. As an electron moves within a molecule, its kinetic energy varies with its position relative to other particles contained in the molecule. If at a certain point,  $\mathbf{r}$ , its energy is equal to the potential it experiences, its average kinetic energy becomes zero and then  $\mathbf{r}$  is called a classical turning point for the electron motion. It has been well justified that, at a turning point, the potential acting on an electron ( $V(\mathbf{r})$ ) is equal to the minus of the first vertical ionization potential ( $I$ ), namely,  $V(\mathbf{r}) = -I$ .<sup>22–24,46</sup> The molecular intrinsic characteristic contour (MICC) can be defined as the collection of all classical turning points. Note that the MICC is of clear physical meaning, as it corresponds to the classical turning point of electron motion within a molecule.

**2.3. Variation of the MICC and the Electron Density Mapped on It during the Formation of the Fluoroethyl Radical.** In this section, we describe the changes of the molecular intrinsic characteristic contour (MICC) and the electron density mapped on it during the formation of  $\text{CH}_2\text{FCH}_2$  from a separate fluorine atom and ethylene.

In addition to the four structures explicitly present on the potential energy surface for the formation of  $\text{CH}_2\text{FCH}_2$ , that is,  $\text{C}_2\text{H}_4$ ,  $\mathbf{I}_{\text{add}}$ ,  $\mathbf{TS}_{\text{add}}$ , and  $\text{CH}_2\text{FCH}_2$  [herein, the geometries optimized at the MP2/6-311++G(3df,3pd) level are used], another two structures are also considered, where F locates above the center of the C–C bond with the perpendicular distances to the molecular plane of ethylene being 8.0 and 5.9 au, respectively, which were obtained by keeping  $R_d$  fixed and optimizing the remaining degrees of freedom at the MP2/6-311++G(3df,3pd) level. To obtain the MICCs of the six structures requires knowledge of the vertical ionization potentials for them, which were calculated at the CCSD(T)/aug-cc-pVDZ level. The results are listed in Table 3. The visualized MICCs as well as the electron density mapped on the contours for the six structures are presented in Figure 4.

To describe the interaction between a fluorine atom and ethylene in more detail, it is necessary to define several parameters. When the contours of the fluorine atom and ethylene remain separated, the straight line passing through the fluorine nucleus and the center of the C–C bond of ethylene has four crossing points with the contours of the fluorine atom and

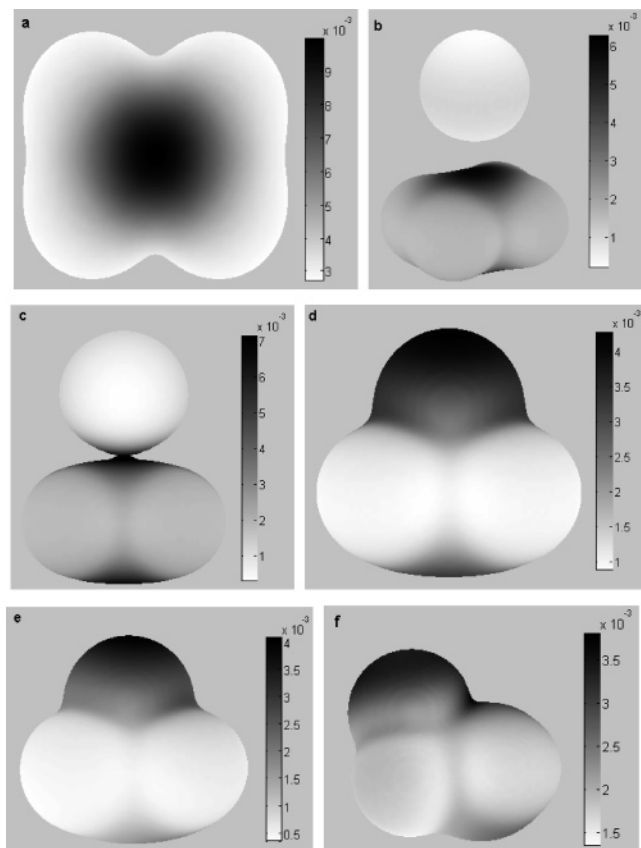


**Figure 4.** MICCs for the structures of interest for the fluorine addition to ethylene with the electron density mapped on them. The magnitude of electron density on the MICC is directly proportional to the gray scale, as shown by the color bar: (a)  $\text{CH}_2\text{CH}_2$ ; (b)  $R_d = 8.0$  au; (c)  $R_d = 5.9$  au; (d)  $\text{TS}_{\text{add}}$ ; (e)  $\text{I}_{\text{add}}$ ; (f)  $\text{CH}_2\text{FCH}_2$ .

**TABLE 4: Parameters Describing the Interaction between F and  $\text{C}_2\text{H}_4$  (in au)**

	$R_d = 8.0$	$R_d = 5.9$	$\text{I}_{\text{add}}$		$R_d = 8.0$	$R_d = 5.9$	$\text{I}_{\text{add}}$
$R_A^{\text{F}}$	3.27	3.06	2.84	$D_A^{\text{F}}$	0.000 25	0.001 28	0.002 52
$R_B^{\text{F}}$	3.78	2.85		$D_B^{\text{F}}$	0.000 27	0.007 10	
$R_C^{\text{E}}$	2.97	3.05		$D_C^{\text{E}}$	0.006 21	0.007 10	
$R_D^{\text{E}}$	2.91	2.92	3.56	$D_D^{\text{E}}$	0.002 11	0.006 82	0.002 18

ethylene, which is in turn marked by A, B, C, and D. The distances from points A and B to the fluorine nucleus are denoted  $R_A^{\text{F}}$  and  $R_B^{\text{F}}$ , respectively. Likewise, the distances from C and D to the center of the double bond of ethylene are referred to as  $R_C^{\text{E}}$  and  $R_D^{\text{E}}$ . The electron densities at the four points are represented by  $D_A^{\text{F}}$ ,  $D_B^{\text{F}}$ ,  $D_C^{\text{E}}$ , and  $D_D^{\text{E}}$  individually. The calculated values of these quantities for the three structures ( $R_d = 8.0$  au,  $R_d = 5.9$  au, and  $\text{I}_{\text{add}}$ ) are listed in Table 4.

Figure 4a presents the molecular intrinsic characteristic contour (MICC) of ethylene and the electron density mapped on it. It can be clearly seen that there is a maximum of electron density on the MICC of ethylene located just above the center of the C–C bond. Surprisingly, according to the results of our ab initio calculations, the fluorine atom locates also above the center of the C–C bond in the prereaction complex ( $\text{I}_{\text{add}}$ ) arising from the association of the fluorine atom to ethylene. Thus, it seems that the fluorine atom tends to attack the electron-rich point on the MICC of ethylene, due to its strong electronegativity.

As the fluorine atom begins to approach ethylene, say, at  $R_d = 8.0$  au, the fluorine atom and ethylene do not affect each other very much, so that the contours of the fluorine atom and

ethylene remain separated, as shown in Figure 4b. The interaction between the fluorine atom and ethylene can be described in two aspects. On one hand, the interaction causes the contours for both of them to expand toward each other. For the fluorine atom,  $R_B^{\text{F}}$  is longer than  $R_A^{\text{F}}$  by 0.51 au; as to ethylene,  $R_C^{\text{E}}$  is 0.06 au longer than  $R_D^{\text{E}}$ . On the other hand, the electron density on the contour of ethylene tends to converge on the side close to the fluorine atom as a response to the presence of the electronegative fluorine atom. As shown in Table 4,  $D_C^{\text{E}}$  is considerable larger than  $D_D^{\text{E}}$  by 0.004 00 au. A similar trend is also observed in the fluorine atom, though not so evident as ethylene, with  $D_B^{\text{F}}$  being 0.000 02 au larger than  $D_A^{\text{F}}$ . Both phenomena can be attributed to the interpolarization effect between fluorine and ethylene. Another interesting phenomenon is that the electron density on the contour of ethylene is larger than that on the contour of fluorine.

As the fluorine atom approaches ethylene, at a distance of about  $R_d = 5.9$  au, the contour of the fluorine atom contacts that of ethylene, as shown in Figure 4c. It can be seen that, at the touching point, the contour of ethylene swells sharply toward the fluorine atom ( $R_C^{\text{E}}$  is longer  $R_D^{\text{E}}$  by 0.13 au). This demonstrates that the fluorine atom strongly attracts the electrons of ethylene toward it. In contrast, the fluorine atom shrinks on the touching side with  $R_B^{\text{F}}$  being 0.21 au shorter than  $R_A^{\text{F}}$ . In addition, around the touching point, the electron density is larger than other places on the MICCs, which is especially evident for the domain of the fluorine atom. As shown in Table 4,  $D_B^{\text{F}}$  is larger than  $D_A^{\text{F}}$  by 0.005 82 au. This indicates that the electrons of ethylene transfer to the fluorine atom to a certain degree.

Figure 4d shows the MICC of  $\text{I}_{\text{add}}$ , where the two contours of the fluorine atom and ethylene fuse into an independent entity. Another evident change of the contour is that the contour shrinks on the backside of the fluorine atom, while on the backside of the ethylene moiety it expands greatly.  $R_A^{\text{F}}$  is shortened by 0.22 au, while  $R_D^{\text{E}}$  is lengthened by 0.64 au relative to that of the previous case ( $R_d = 5.9$  au). Furthermore, the electron distribution on the MICC separates the contour into two distinct domains with the electron density on the fluorine domain being evidently larger than that on the ethylene domain, contrary to the previous case. This indicates that electron transfer from the ethylene to the fluorine occurs, which makes the fluorine encompass extra electrons and ethylene deficient in electrons relative to their separate states.

The contour of  $\text{TS}_{\text{add}}$  is shown in Figure 4e. Comparison of the contour of  $\text{TS}_{\text{add}}$  to that of  $\text{I}_{\text{add}}$  shows that  $\text{TS}_{\text{add}}$  is very similar to  $\text{I}_{\text{add}}$  in both the shape of the MICC and the electron density on it. This is consistent with the conclusion we obtained above that the transition structure  $\text{TS}_{\text{add}}$  is reactant-like.

At the product stage, the contour of  $\text{CH}_2\text{FCH}_2$ , as shown in Figure 4f, is quite distinct from that of the transition structure  $\text{TS}_{\text{add}}$ . The convexity of the fluorine domain is more prominent than that of  $\text{TS}_{\text{add}}$ , corresponding to the complete formation of the C–F bond. The contour of  $\text{CH}_2\text{FCH}_2$  shrinks inward on the backside of the ethylene moiety in response to the weakening of the C–C bond, due to the conversion of the double bond to a single bond.

## Conclusions

A thorough study has been conducted on the substitution reaction between a fluorine atom and ethylene. The geometrical parameters for all structures involved in the title reaction were optimized at different high theoretical levels. The obtained results show that the MP2 method with Pople's series of basis

sets [6-31G(d,p), 6-311++G(d,p), and 6-311++G(3df,3pd)] yields similar geometrical structures, while the MP2/aug-cc-pVDZ model tends to overestimate bond lengths. In addition, the geometrical parameters of the transition structures involving bond making or breaking and the weakly bound structures appear to be more sensitive to the theoretical levels than most equilibrium structures.

The reaction mechanism for the title reaction was discussed primarily on the basis of the calculation performed at the CCSD-(T)/aug-cc-pVDZ//CCSD/6-31G(d,p) level including the ZPE correction calculated at the MP2/6-311++G(d,p) level. According to our calculations, the fluorine atom and ethylene form the prereaction complex ( $\mathbf{I}_{\text{add}}$ ) in the entrance channel for the title reaction, rather than reach directly the transition structure  $\mathbf{TS}_{\text{add}}$  for fluorine addition to ethylene. The involvement of  $\mathbf{I}_{\text{add}}$  with  $C_{2v}$  symmetry may be responsible for the experimentally observed regioselectivity for the formation of a collision complex between a fluorine atom and ethylene.<sup>1</sup> Subsequently, the prereaction complex ( $\mathbf{I}_{\text{add}}$ ) evolves into a fluoroethyl radical nearly without an energy barrier with an exothermicity of 41.49 kcal/mol. The high exothermicity makes the fluoroethyl radical chemically active, which can further decompose into H and  $\text{CH}_2\text{-CHF}$ , with an energy of 10.33 kcal/mol released. In addition to the direct hydrogen departing from the carbon atom of the fluoroethyl radical, an indirect pathway,  $\text{CH}_2\text{FCH}_2' \rightarrow \mathbf{TS}_{\text{Hshift}} \rightarrow \text{CH}_3\text{CHF} \rightarrow \mathbf{TS}_{\text{dep2}} \rightarrow \text{H} + \text{CH}_2\text{CHF}$ , is also found to be energetically feasible, which has not been reported before.

In terms of the model of the MICC and the electron density mapped on it, the formation of  $\text{CH}_2\text{FCH}_2$  from a separate fluorine atom and ethylene is described pictorially. As the fluorine atom approaches ethylene, the contours tend to swell toward each other, until they fuse into an entity. At the same time, the electron density on both contours gathers on their close sides, as a result of the interpolarization effect between them. Additionally, the MICC and the electron density mapped on the contour for  $\mathbf{TS}_{\text{add}}$  resemble that of  $\mathbf{I}_{\text{add}}$  but are evidently distinct from that of  $\text{CH}_2\text{FCH}_2$ , which is consistent with the result of our ab initio study that the transition structure  $\mathbf{TS}_{\text{add}}$  is reactant-like. This provides an intuitional picture for describing this chemical reaction.

**Acknowledgment.** This research was supported by the National Science Foundation of China (Grant No. 20073018). The authors are very grateful to Prof. E. R. Davidson for his providing the MELD program and other kinds of help.

## References and Notes

- (1) Parson, J. M.; Lee, Y. T. *J. Chem. Phys.* **1972**, *56*, 4658.
- (2) Parson, J. M.; Shobatake, K.; Lee, Y. T.; Rice, S. A. *J. Chem. Phys.* **1973**, *59*, 1402.
- (3) Shobatake, K.; Parson, J. M.; Lee, Y. T.; Rice, S. A. *J. Chem. Phys.* **1973**, *59*, 1416.
- (4) Farrar, J. M.; Lee, Y. T. *J. Chem. Phys.* **1976**, *65*, 1414.
- (5) Benson, S. W. *Thermodynamical Kinetics*; Wiley: New York, 1968.
- (6) Moehlmann, J. G.; Gleaves, J. T.; Hudgens, J. W.; McDonald, J. D. *J. Chem. Phys.* **1974**, *60*, 4790.
- (7) Zvijac, D. J.; Mukamel, S.; Ross, J. *J. Chem. Phys.* **1977**, *67*, 2007.
- (8) Hase, W. L.; Bhalla, K. C. *J. Chem. Phys.* **1981**, *75*, 2807.
- (9) Clark, D. T.; Scanlan, I. W. *Chem. Phys. Lett.* **1978**, *55*, 102.
- (10) Kato, S.; Morokuma, K. *J. Chem. Phys.* **1980**, *72*, 206.
- (11) (a) Schlegel, H. B. *J. Phys. Chem.* **1982**, *86*, 4878. (b) Schlegel, H. B.; Bhalla, K. C.; Hase, W. L. *J. Phys. Chem.* **1982**, *86*, 4883.
- (12) Sekušak, S.; Liedl, K. R.; Sabljčić, A. *J. Phys. Chem. A* **1998**, *102*, 1583 and ref 7 therein.
- (13) Braña, P.; Menéndez, B.; Fernández, T.; Sordo, J. A. *J. Phys. Chem. A* **2000**, *104*, 10842.
- (14) Bader, R. F. W. *Atoms in Molecules: A Quantum Theory*; Clarendon: Oxford, U.K., 1990.
- (15) (a) Chesnut, D. B. *J. Phys. Chem. A* **2003**, *107*, 4307. (b) Cubero, E.; Orozco, M.; Hobza, P.; Luque, F. J. *J. Phys. Chem. A* **1999**, *103*, 6394. (c) Exner, K.; Schleyer, P. v. R. *J. Phys. Chem. A* **2001**, *105*, 3407. (d) Zeng, X.; Davico, G. E. *J. Phys. Chem. A* **2003**, *107*, 11565. (e) Vila, A.; Mosquera, R. *J. Phys. Chem. A* **2000**, *104*, 12006. (f) Zhurova, E. A.; Tsirelson, V. G.; Stash, A. I.; Pinkerton, A. A. *J. Am. Chem. Soc.* **2002**, *124*, 4574.
- (16) (a) Sjöberg, P.; Politzer, P. *J. Phys. Chem.* **1990**, *94*, 3959. (b) Politzer, P.; Murray, J. S.; Concha, M. C. *Int. J. Quantum Chem.* **2002**, *88*, 19. (c) Politzer, P.; Abu-awwad, F.; Murray, J. S. *Int. J. Quantum Chem.* **1998**, *69*, 607.
- (17) Ehresmann, B.; Martin, B.; Horn, A. H. C.; Clark, T. *J. Mol. Model.* **2003**, *9*, 342.
- (18) (a) Mezey, P. G. *J. Chem. Inf. Comput. Sci.* **1992**, *32*, 650. (b) Walker, P. D.; Maggiora, G. M.; Johnson, M. A.; Petke, J. D.; Mezey, P. G. *J. Chem. Inf. Comput. Sci.* **1995**, *35*, 568.
- (19) (a) Walker, P. D.; Mezey, P. G. *J. Am. Chem. Soc.* **1993**, *115*, 12423. (b) Walker, P. D.; Mezey, P. G. *J. Am. Chem. Soc.* **1994**, *116*, 12022.
- (20) Mezey, P. Z.; Zimpel, Z.; Warburton, P.; Walker, P. D.; Irvine, D. G.; Dixon, D. G.; Greenberg, B. Mezey, *J. Chem. Inf. Comput. Sci.* **1996**, *36*, 602.
- (21) Mezey, P. G. *J. Mol. Model.* **2000**, *6*, 150.
- (22) Yang, Z. Z.; Zhao, D. X. *Chem. Phys. Lett.* **1998**, *292*, 387.
- (23) Yang, Z. Z.; Zhao, D. X.; Wu, Y. *J. Chem. Phys.* **2004**, *121*, 3452.
- (24) (a) Gong, L. D.; Zhao, D. X.; Yang, Z. Z. *THEOCHEM* **2003**, *636*, 57. (b) Yang, Z. Z.; Gong, L. D.; Zhao, D. X.; Zhang, M. B. *J. Comput. Chem.* **2005**, *26*, 35.
- (25) Møller, C.; Plesset, M. S. *Phys. Rev.* **1934**, *46*, 618.
- (26) Hehre, W. J.; Radom, L.; Schleyer, P. v. R.; Pople, J. A. *Ab initio Molecular Orbital Theory*; Wiley: New York, 1986.
- (27) Dunning, T. H., Jr. *J. Chem. Phys.* **1989**, *90*, 1007. (b) Kendall, R. A.; Dunning, T. H., Jr. *J. Chem. Phys.* **1992**, *96*, 6796. (c) Woon, D. E.; Dunning, T. H., Jr. *J. Chem. Phys.* **1993**, *98*, 1358.
- (28) Purvis, G. D.; Bartlett, R. J. *J. Chem. Phys.* **1982**, *76*, 1910.
- (29) Scuseria, G. E.; Janssen, C. L.; Schaeffer, H. F., III. *J. Chem. Phys.* **1989**, *89*, 7392.
- (30) Scuseria, G. E.; Schaeffer, H. F., III. *J. Chem. Phys.* **1989**, *90*, 3700.
- (31) Pople, J. A.; Head-Gordon, M.; Raghavachari, K. *J. Chem. Phys.* **1987**, *87*, 5968.
- (32) Pople, J. A.; Frisch, M. J.; Trucks, G. W.; Schlegel, H. B.; Scuseria, G. E.; Robb, M. A.; et al. *Gaussian 98*, revision A.7; Gaussian, Inc.: Pittsburgh, PA, 1998.
- (33) Davidson, E. R. MELD Program Description in MOTECC; ESCOM: New York, 1990.
- (34) <http://www.rocq.inria.fr/scilab>, INRIA (Insitut National de Recherche en Informatique et en Automatique) and ENPC (L'Ecole Natioanle des Ponts et Chaussées), SCILAB 2.6, 2002.
- (35) Chen, K. S.; Krusic, P. J.; Meakin, P.; Kochi, J. K. *J. Phys. Chem.* **1974**, *78*, 2014.
- (36) Stanton, J. F. *J. Chem. Phys.* **1994**, *101*, 371.
- (37) Chuang, Y.-Y.; Coitiño, E. L.; Truhlar, D. G. *J. Phys. Chem. A* **2000**, *104*, 446.
- (38) (a) Fukui, K. *J. Phys. Chem.* **1970**, *74*, 4161. (b) Fukui, K.; Kato, S.; Fujimoto, H. *J. Am. Chem. Soc.* **1975**, *97*, 1.
- (39) (a) Gonzalez, C.; Schlegel, H. B. *J. Chem. Phys.* **1989**, *90*, 2154. (b) Gonzalez, C.; Schlegel, H. B. *J. Phys. Chem.* **1990**, *94*, 5523.
- (40) Selçuki, C.; Aviyente, V. *J. Mol. Model.* **2001**, *7*, 398.
- (41) Braña, P.; Sordo, J. A. *J. Comput. Chem.* **2003**, *24*, 2044.
- (42) Singleton, D. L.; Cvetanovic, R. J. *J. Am. Chem. Soc.* **1976**, *98*, 6812.
- (43) Mozurkewich, M.; Benson, S. W. *J. Phys. Chem.* **1984**, *88*, 6429.
- (44) Durana, J. F.; McDonald, J. D. *J. Chem. Phys.* **1975**, *64*, 2518.
- (45) Chen, Y.; Rauk, A.; Tschuikow-Roux, E. *J. Chem. Phys.* **1990**, *93*, 6620.
- (46) (a) Yang, Z. Z.; Davidson, E. R. *Int. J. Quantum Chem.* **1996**, *62*, 47. (b) Yang, Z. Z.; Niu, S. Y. *Chin. Sci. Bull.* **1991**, *2*, 159. (c) Zhang, M. B.; Zhao, D. X.; Yang, Z. Z. *J. Theor. Comput. Chem.* **2005**, *4*, 281.